ELSEVIER

Biophysical Chemistry 108 (2004) 259–271

Biophysical Chemistry

www.elsevier.com/locate/bpc

Hydrodynamic bead modelling of the 2:1 p50–IκBγ complex

Michaela Smolle[a,b], Ronald T. Hay[c], Olwyn Byron[a,*]

[a]*Division of Infection and Immunity, Joseph Black Building, University of Glasgow, Glasgow G12 8QQ, Scotland, UK*
[b]*Division of Biochemistry and Molecular Biology, Davidson Building, University of Glasgow, Glasgow G12 8QQ, Scotland, UK*
[c]*Biomolecular Sciences Building, School of Biology, University of St. Andrews, The North Haugh, St. Andrews KY16 9ST, Scotland, UK*

Abstract

NFκB is an important and ubiquitous transcription factor formed by various homo- and heterodimers of the NFκB family. The active transcription factor regulates genes involved in immune, inflammatory and survival responses. Specificity in gene regulation is achieved, at least in part, by the distinct DNA binding preferences of the various homo- and heterodimers and by the complex pathways that lead to signal-induced degradation of the IκB inhibitors. Analytical ultracentrifugation and hydrodynamic bead modelling were used to model the solution structures of the NFκB family member p50, its inhibitor IκBγ and their complex. Sedimentation equilibrium (SE) and sedimentation velocity (SV) data show that p50 is a dimer in solution with a sedimentation coefficient consistent with a conformation intermediate between the closed conformation observed in the crystal structure of the p50 (N-terminal domain)–p65 heterodimer complexed with IκBα and the open conformation adopted by p50 when bound to DNA. SE and SV data show that IκBγ is a monomer in solution and is prone to aggregation over time. p50 forms a 2:1 stoichiometric complex with IκBγ in solution with a sedimentation coefficient consistent with a closed conformation for the p50 dimer.

Keywords: Analytical ultracentrifugation; Hydrodynamic bead modelling; p50; IκBγ; Gene regulation

1. Introduction

1.1. The NFκB/Rel family

The NFκB/Rel family of eukaryotic transcription factors controls a wide variety of inducible genes involved in inflammation, activation of immune cells, inhibition of apoptosis, cell proliferation, cell migration and repair, as well as its own gene expression and even that of viruses, e.g. human immunodeficiency virus or herpes [1–4]. Abnormal activity of NFκB homo- or heterodimers is associated with a range of diseases such as Hodgkin's disease, melanoma, various lymphomas, myelomas, leukaemia, carcinomas and adenocarcinomas, and also with rheumatoid arthritis, asthma, arteriosclerosis and Alzheimer's disease [3].

NFκB family members are characterised by their possession of the Rel homology domain that is responsible for DNA binding, dimerisation and interaction with inhibitor proteins. The five members of the mammalian NFκB/Rel family fall into

*Corresponding author. Tel.: +44-141-330-3752; fax: +44-141-330-4600.
E-mail address: o.byron@bio.gla.ac.uk (O. Byron).

0301-4622/04/$ - see front matter © 2003 Elsevier B.V. All rights reserved.
doi:10.1016/j.bpc.2003.10.032

two subgroups: p65, c-Rel and RelB contain transcriptional activation domains while p50 and p52 lack the activation domain [4]. p50 and p52 can be generated by proteolytic processing of their respective longer precursor proteins p105 and p100 [1,3,4] as well as by a novel co-translational mechanism [5,6].

1.2. Regulation of NFκB activity

Members of the NFκB/Rel family form various homo- and heterodimers that have distinct affinities for different DNA binding (κB) sites. Furthermore, their cellular distribution and activity are controlled by association with and inhibition by proteins of the IκB family [4]. The IκB family currently encompasses six proteins: IκBα, -β and -ε are stimulus-dependent regulators of NFκB, while IκBδ, -γ and Bcl-3 have other functions [7]. All IκB proteins, however, consist of a varying number of ankyrin repeats which are known protein–protein interaction motifs [3,8].

1.3. Diversity within the IκB family

Many agents that activate NFκB do so by inducing IκB phosphorylation by the IκB kinase (IKK) complex, which contains two catalytic subunits IKK1 (or IKKα) and IKK2 (or IKKβ) and a structural subunit IKKδ. IκB phosphorylation targets the protein for ubiquitination and proteasome-mediated degradation. p105 can also function as an IκB via the ankyrin repeats at its C-terminus which retain bound p50, c-Rel and RelA in the cytoplasm. The C-terminal ankyrin repeats of p105 can also be generated as a separate protein (IκBδ) as a result of alternative splicing of the *NFκB1* gene in lymphoid cells in mice. Analysis of mice that are unable to produce the C-terminal ankyrin repeat containing half of p105 but which still express p50 has revealed an important role for the C-terminus of p105 in NFκB regulated control of the inflammatory response [9]. p105 levels are controlled by two distinct proteolytic pathways in which p105 can either be processed to p50 or completely degraded. In response to certain stimuli, p105 is phosphorylated by IKK and, after signal-induced ubiquitination, degraded by the proteasome. This leads to p105 degradation rather than processing, which is normally constitutive [10].

Different IκB proteins are thought to interact differently with individual NFκB homo- and heterodimers thus accounting for the subtle control of NFκB activation. Most studies so far have focused on IκBα [11–13] whose structure in complex with the p65–p50 heterodimer has been solved by X-ray crystallography [14,15]. The latter binds only one of two nuclear localisation sequences (NLS) present in IκBα, which allows for nuclear translocation of NFκB–IκBα complexes. However, the presence of nuclear export sequences in IκBα ensure that imported complexes are rapidly exported back to the cytoplasm. Although rapid shuttling of IκBα/p50–p65 takes place in unstimulated cells, the equilibrium reached ensures that IκBα/p50/p65 is predominantly cytoplasmic [16,17]. IκBβ, on the other hand, binds both NLSs available and thus ensures complete retention of complexed molecules in the cytoplasm [18]. IκBγ contains seven ankyrin repeats and it has been proposed that it binds NFκB in such a way that it contacts residues required for protein–DNA interactions and thus prevents DNA binding of NFκB [19].

1.4. Structural information to date

The structures of several NFκB homo- and heterodimers, including the p50 homodimer complexed with κB sites, have been solved by X-ray crystallography [4,20–23]. The p50/p65–IκBα complex has also been characterised, although truncated versions of all proteins were used in the crystallisation process [14,15]. Interestingly, the N-terminal domains of p50 and p65 in these two structures have virtually the same conformation but different orientations, having undergone an apparent 180° rotation and 40 Å translation when bound to the inhibitor. Apart from IκBα, Bcl-3 is the only other IκB protein whose structure has been solved [24].

To date, there are no high-resolution structures of uncomplexed homo- and heterodimers of NFκB. Furthermore, there is biochemical evidence for differences in the interaction of NFκB with differ-

ent members of the IκB family [11,12,18,19]. However, as yet there is no way to establish a structural basis for these differences since the structure of Bcl-3 was determined in its uncomplexed form. In this paper, we try to bridge this gap by reporting the low-resolution solution structures of p50, IκBγ and their complex. In particular, we focus on the orientation of the p50 N-terminal domain when uncomplexed and, in addition, map the interaction of p50 with IκBγ. Since IκBγ is thought to prevent DNA-binding of p50 completely, their interactions are necessarily different when compared to the p65–p50–IκBα complex.

2. Materials and methods

2.1. Proteins

IκBγ and p50 were both expressed and purified as described previously [19,25,26]. p50 included residues 35–381 and IκBγ residues 537–809 of their common precursor protein p105 encoded by the *NFκB1* gene. Purity of the proteins was checked using standard SDS-PAGE analysis [27].

2.2. Analytical ultracentrifugation

Prior to sedimentation velocity (SV) analytical ultracentrifugation (AUC) analysis, p50 and IκBγ were dialysed against a 1000-fold volume excess of 50 mM Tris, 300 mM NaCl, 2 mM DTT, pH 8.0 over a period of 36 h with two complete changes of solvent. After extended periods of time, p50 and IκBγ were observed to precipitate. Therefore, prior to the lengthier procedure of sedimentation equilibrium (SE) AUC, buffer equilibration was achieved via more rapid buffer exchange using a PD-10 (Amersham Biosciences) Sephadex G-25 desalting column. AUC studies were performed using Optima XL-I and XL-A analytical ultracentrifuges (Beckman-Coulter, Palo Alto, CA). SV experiments were conducted at 45 k rpm using both absorbance and interference optics with double-channel centrepieces. Absorbance data were acquired in continuous mode (5 replicates, 0.003 cm step size). The wavelengths of the incident light were set to 280 nm for p50 and p50:IκBγ mixtures, and 278 nm for IκBγ.

SV data were analysed using the program SEDFIT [28] that directly fits the velocity profiles. The non-interacting species model was used with three species representing p50, IκBγ and their complex. High-resolution fits were conducted over the range 0.1–20 S in sedimentation coefficient space to cover all conceivable species. The best fits were obtained with a frictional ratio of 1.2 for all species (the fits were not improved by floating the frictional ratio). The sedimentation coefficient and diffusion coefficient of each species were floated and all six data sets (acquired at different mixing ratios of p50 and IκBγ) were fitted to yield the sedimentation coefficients for the separate species that were corrected for the effects of temperature, buffer density and viscosity to generate the coefficients at 20 °C in water. Size-distribution analysis ($c(s)$ vs. s) was also performed using SEDFIT to describe the heterogeneity of the sedimenting solute.

For SE analysis IκBγ and p50 were loaded into Yphantis-type six- and double-channel centrepieces, respectively. Absorbance data were acquired in step mode (10 replicates, 0.001 cm step size). Equilibrium solute distributions were obtained at the following rotor speeds: p50 (15, 18 and 20 k rpm); IκBγ (17 and 23 k rpm); p50–IκBγ (10, 13.5 and 17 k rpm). SE data were analysed with Beckman XL-A–XL-I software based on Microcal ORIGIN 6.0 using the self-association model.

2.3. Modelling the p50 homodimer

We wanted to construct a model for the p50 homodimer in the conformation it would adopt were it to be inhibited by IκBγ. Protein data bank (PDB) ([29] (http://www.rcsb.org/pdb/)) file 1NFI comprises coordinates for a p50–p65 heterodimer complexed with IκBα in which the C-terminal domain of p50 is missing. Thus, it was not possible to ascertain from these data the likely conformation of p50 in its inhibited state. Instead, the superimposition tools included in the program DEEPVIEW [30] were used for complex reconstruction using PDB file 1NFI as follows: both the N-terminal domain of p50 (from PDB file 1NFI) and its C-terminal domain (from PDB file 1NFK) were

superimposed onto the corresponding domains of p65 as found in PDB file 1NFI. The resulting construct was then copied and the copy superimposed onto the existing p50 C-terminal domain of 1NFI in order to generate the remaining half of the dimer. We use 'open' and 'closed' to refer to the two extremes of p50 conformation, whereby 'open' refers to p50 as found in the DNA-bound complex while 'closed' describes the p50 conformation observed in the NFκB-inhibitor complex.

2.4. Modelling IκBγ

A high-resolution model of IκBγ was constructed from the structure of IκBα (PDB accession code 1NFI) by attaching a duplicated sixth ankyrin repeat to the molecule's C-terminus. However, the 40 C-terminal residues of IκBγ were not accounted for in this model. Homology-based modelling was not possible because there are few primary sequence homologues to this region and none for which an atomic structure has been solved. Instead, the secondary structure of the C-terminus predicted using the JPRED server [31] was folded into a tertiary structure using the program DRAGON [32]. DRAGON was run 20 times generating two distinct families of structures. Structures within each family were ranked according to bond (between neighbouring residues in the primary sequence), non-bond (between non-neighbouring residues), external restraint and secondary structure scores. The highest scoring structure was used to represent each of the families.

2.5. Hydrodynamic modelling

The program AtoB [33,34] can transform atomic coordinates into bead models comprising spheres of a radius dependent on the 'resolution' chosen. Models were generated for the p50 homodimer ($(p50)_2$) and IκBγ with beads of radius 3.5 Å. A number of residues of p50 are not resolved in the atomic structure and were thus missing from the initial hydrodynamic bead model. The mass and volume occupied by residues 1–4, 246–248 and 356–381 in p50 were calculated from the molecular weight and partial specific volume of p50 and thus the number of beads correspondingly required to represent these residues determined. Four beads for residues 1–4, 2 beads for residues 246–248 and 22 beads for residues 356–381 were joined onto the existing bead model 'manually' using the program MACBEADS (written by Dr Dan Thomas, then at the National Centre for Macromolecular Hydrodynamics (NCMH), University of Leicester, obtainable on request from the NCMH, Nottingham (http://www.nottingam.ac.uk/ncmh/unit/software.html)). Since the conformation of residues 356–381 is unknown, three structural extremes—where the peptide assumes either a straight, bent or globular conformation—were modelled and assessed separately.

The C-terminal peptide of IκBγ modelled using DRAGON [32] (above) was transformed into beads using AtoB [33,34] and then built onto the existing bead model of IκBγ (IκBα plus the extra ankyrin repeat) using MACBEADS. Only one of the C-terminal peptide structures of the IκBγ model was used since the second DRAGON structure could not be attached to the rest of the molecule without causing steric clashes.

Bead models for the $(p50)_2$–IκBγ complex were obtained by superposition of the individual bead models of $(p50)_2$ and IκBγ using MACBEADS. The complex was modelled with $(p50)_2$ in two distinct conformations: the inhibitor-bound, 'closed' conformation—as seen in 1NFI—and the DNA-bound, 'open' conformation determined by Müller et al. (PDB accession code 1NFK) [23].

Anhydrous sedimentation coefficients (s) for all bead models were calculated using the program HYDRO [35]. In order to compare the HYDRO output with the values for s obtained experimentally, a correction was made for hydration (see e.g. [34]) using a value of 0.4 g water/g protein.

3. Results

3.1. p50 is a dimer in solution

SE solute distributions for p50 at three rotor speeds were well fitted with the equation for a single, thermodynamically ideal species, yielding the apparent whole cell weight average molecular weights ($M_{w,app}$) summarised in Fig. 1. The molar mass of p50 calculated from its amino acid

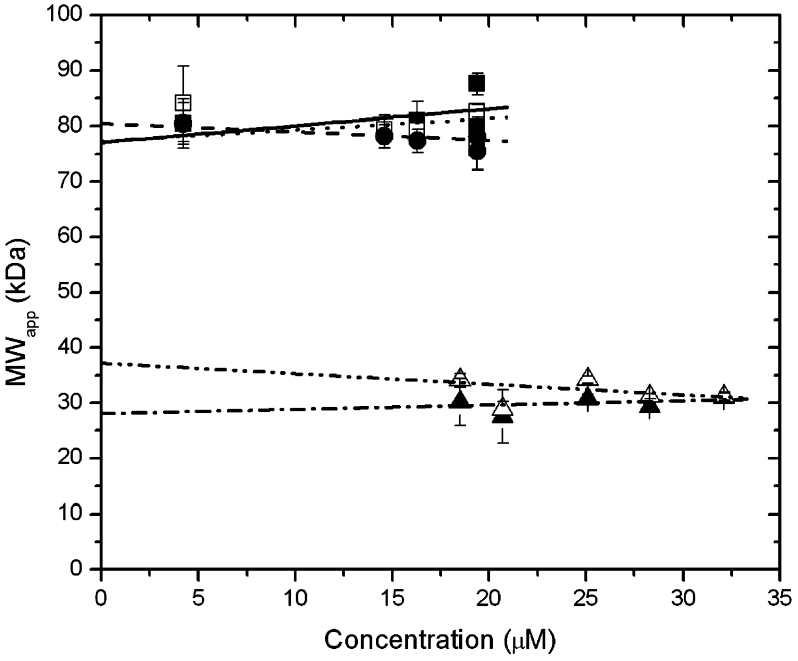

Fig. 1. Apparent whole cell weight average molecular weight ($M_{w,app}$) as a function of loading concentration (in monomer molar units) extrapolated to infinite dilution for p50 (data were acquired at rotor speeds of 15 k rpm (filled squares, solid line); 18 k rpm (open squares, dotted line); 20 k rpm (filled circles, dashed line)) and IκBγ (data were acquired at rotor speeds of 17 k rpm (filled triangles, dot-dashed line); 23 k rpm (open triangles, double dot-dashed line)). For comparison, p50 dimer would have a molecular weight of 77.6 kDa; the molecular weight of IκBγ is 29.4 kDa.

sequence is 38 909 Da; the data in Fig. 1 extrapolate to give molecular weights at infinite dilution ($M^0_{w,app}$) of 77.2 kDa (at 15 and 18 k rpm) and 80.5 kDa (at 20 k rpm). These data suggest that p50 is a dimer in solution over the concentration range studied. This is consistent with the sedimentation coefficients determined for p50. Size-distribution analysis of the SV data gave a single peak centered about an apparent sedimentation coefficient of 4.90 S (Fig. 2) and the SV profiles were well fitted with a single species model. Extrapolation to infinite dilution of the concentration dependence of $s_{20,w}$ (Fig. 3) gives $s^0_{20,w}=4.19$ S (absorbance data) and 4.45 S (interference data). The maximum possible sedimentation coefficient for monomeric p50 can be calculated using standard equations to be 3.99 S (i.e. for an anhydrous sphere with the same mass and partial specific volume as p50); including 0.4 g/g hydration this value decreases to 3.43 S. The corresponding values for a spherical dimer are 6.34 S (anhydrous) and 5.45 S (0.4 g/g hydration). Therefore, according to SV data, p50 is not monomeric; oligomers higher than dimer appear unlikely as their sedimentation coefficients would far exceed the measured value. Thus as a dimer $(p50)_2$ must be not only hydrated but also asymmetrical.

Sedimentation coefficients were calculated for bead models of the p50 homodimer in open and closed conformations with three extreme representations of the 26 most C-terminal residues (Fig. 4). The results are summarised in Table 1. For both the 'open' and 'closed' $(p50)_2$ models the globular tail conformation gives hydrated sedimentation coefficients (4.03 and 4.40 S, respectively) most consistent with the experimentally determined values (4.19 S (absorbance data) and 4.45 S (interference data)). Of the two homodimer conformations, the closed form agrees more closely with the experimental data, although on the

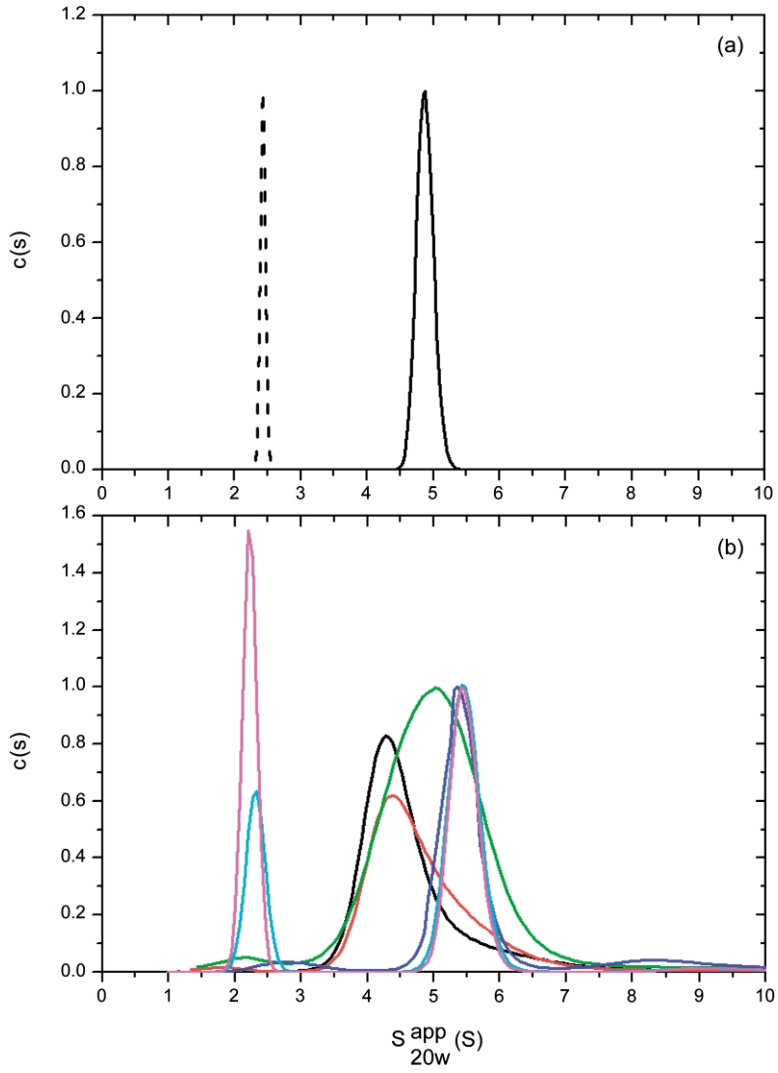

Fig. 2. Size-distribution ($c(s)$) converted to standard conditions for (a) p50 and IκBγ and (b) mixtures of the two. p50 absorbance data at 280 nm, loading concentration (in monomer molar units) $c=43.5$ μM (solid line (black)); IκBγ absorbance at 278 nm, $c=46.1$ μM (dashed line); absorbance data (at 280 nm) for mixtures of p50 and IκBγ at molar ratios (p50:IκBγ) of 4:1 (red), 3:1 (black), 2:1 (green), 1:1 (blue), 1:2 (cyan) and 1:3 (pink).

basis of these data alone it is not possible to conclude that $(p50)_2$ is definitely in a closed conformation; there will be other conformations consistent with the measured sedimentation coefficient.

3.2. IκBγ is a monomer in solution

SE data for IκBγ acquired at 17 k rpm were well fitted with the model for a single, thermodynamically ideal species, yielding $M^0_{w,app}=28.0$ kDa. However, the equilibrium solute distribution obtained subsequently at the higher rotor speed of 23 k rpm was poorly fitted with this model and gave a higher $M^0_{w,app}=37.2$ kDa, indicative of the formation of aggregate over the course of the AUC run. Certainly the same tendency was observed during small-angle X-ray scattering studies to an extent that precluded the acquisition of scattering

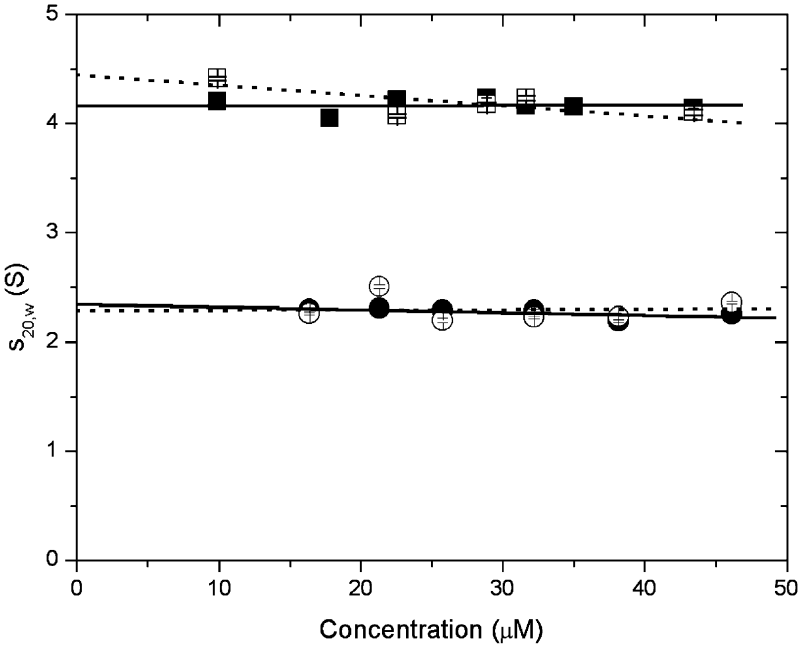

Fig. 3. Extrapolation to zero concentration of sedimentation coefficients for p50 (interference data (open squares, dashed line); absorbance data at 280 nm (closed squares, solid line)) and IκBγ (interference data (open circles, dashed line); absorbance data at 278 nm (closed circles, solid line)).

curves of high enough quality for dummy atom or dummy residue modelling (Section 4). Size-distribution analysis of the SV data gave a single peak centered about an apparent sedimentation coefficient of 2.4 S (Fig. 2) and the SV profiles were well fitted with a single species model. Extrapolation to infinite dilution of the concentration dependence of $s_{20,w}$ (Fig. 3) gives $s^0_{20,w}=2.35$ S (absorbance data) and 2.38 S (interference data). The sedimentation coefficients calculated (using HYDRO [35]) for the IκBγ model (Fig. 5) whose construction is described in Section 2 are 2.79 S (anhydrous) and 2.40 S (hydrated) (Table 1). Thus, the model is entirely consistent with the experimental data.

3.3. p50 forms a 2:1 stoichiometric complex with IκBγ in solution

By performing SE analysis for different mixtures of $(p50)_2$ and IκBγ at different molar ratios, we hoped to observe a peak in $M_{w,app}$ for the mixture with the optimal stoichiometry (provided we are working somewhat above the K_d for the interaction) when most of the species in solution would have associated into complexes. At mixing ratios for which uncomplexed molecules remain in solution, $M_{w,app}$ will be depressed. The reduced SE data are shown in Fig. 6. The decrease in $M_{w,app}$ with increasing rotor speed could be indicative of the formation of high molecular weight aggregate that is steeply distributed at higher speed equilibrium and is thus effectively excluded from subsequent analysis. Higher rotor speed data were acquired after the lowest speed data. Given that there is no evidence of aggregate species in the SV data (below) we presume that the aggregate has formed with time. Thus, in what follows we refer only to the earliest acquired SE data (obtained at 10 k rpm). The hoped-for peak in $M_{w,app}$ is observed at a mixing ratio of 3:1 (p50 monomer: IκBγ monomer). A complex with this stoichiometry would have a molecular weight of 146.1 kDa instead of the 117 kDa observed at the

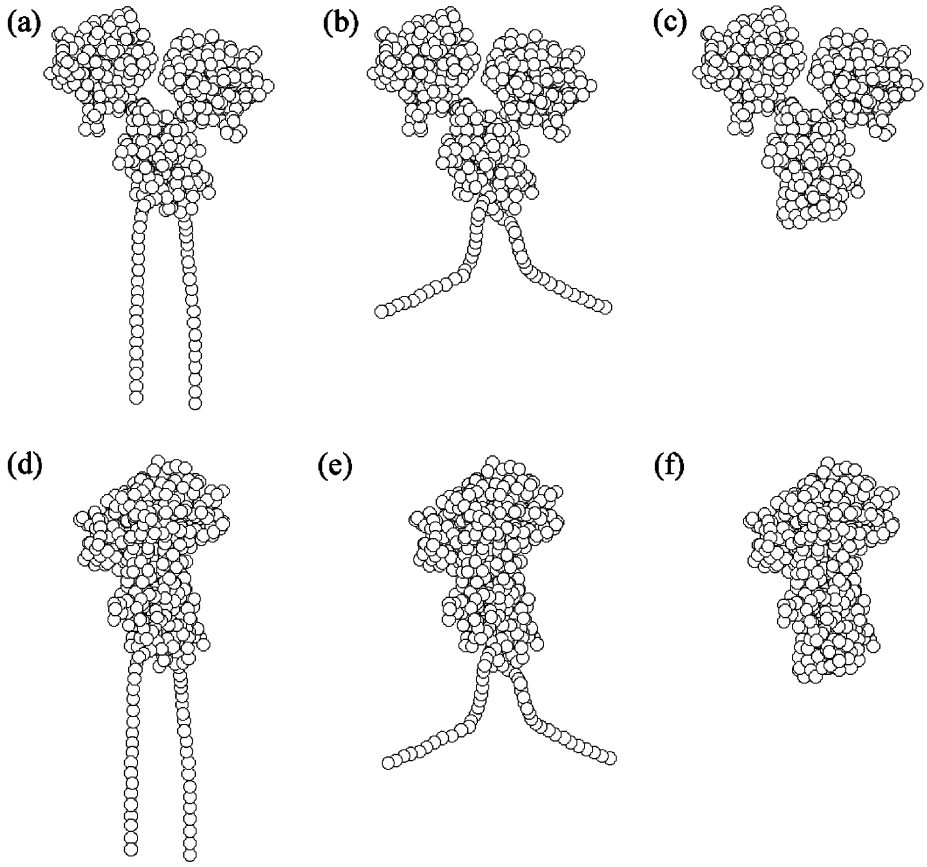

Fig. 4. Bead models for p50 in the open (a–c) and closed (d–f) conformations with the C-terminus domain modelled in three extreme conformations: extended (a, d), bent (b, e) and globular (c, f).

lowest rotor speed. The molecular mass of the 2:1 complex would be 107.2 kDa. Instead of observing a real decrease in $M_{w,app}$ at mixing ratios for which IκBγ is in excess, the mass remains relatively stable. The abscissa axis in Fig. 6 represents the total protein concentration (albeit weighted by the respective extinction coefficients of the two proteins: calculated to be 19 934 and 15 908 cm^2/mole for p50 and IκBγ, respectively). Thus, although IκBγ is in excess, it also acts to increase the total protein concentration and will drive the hetero-association towards complex formation. The 1:1, 1:2 and 1:3 mixing ratio data obtained at a rotor speed of 10 k rpm give $M_{w,app} \approx 112$ kDa, very close to the molecular weight of the 2:1 complex. It is therefore possible that the 2:1 mixing ratio was established at too low an overall protein concentration to ensure complete formation of the complex. Certainly none of the masses in Fig. 6 suggests a complex of 3:1 or 4:1 but rather 2:1. Two stoichiometric complexes are biologically plausible: the 2:1 (107.2 kDa) and the 2:2 (136.6 kDa, equivalent to 1:1 in Fig. 6). Our SE data point towards the formation of the 2:1 complex in solution.

A clearer picture emerges from the SV data for which the size-distribution analysis is shown in Fig. 2. At p50 monomer:IκBγ monomer ratios of 4:1 and 3:1, only one significant (asymmetrical) peak is observed at an apparent sedimentation coefficient ($s^{app}_{20,w}$) just below that of $(p50)_2$. At a mixing ratio of 2:1 the peak broadens, becomes

Table 1
Sedimentation coefficients calculated for hydrodynamic models of p50, IκBγ and their complex (s_{HYDRO}) compared with measured values ($s^0_{20,w}$)

	$(p50)_2$ conformation	p50 C-terminus	s_{HYDRO} (S)		$s^0_{20,w}$ (S)	
			Anhyd[a]	Hyd[b]	Abs[c]	Int[c]
$(p50)_2$	Closed	Straight	4.06	3.49	4.19	4.45
		Bent	4.10	3.52		
		Globular	5.11	4.40		
$(p50)_2$	Open	Straight	3.90	3.35		
		Bent	3.96	3.41		
		Globular	4.69	4.03		
IκBγ			2.79	2.40	2.38	2.35
$(p50)_2$–IκBγ	Closed	Globular	6.17	5.31	5.51	5.49
	Open	Globular	6.00	5.16	5.51	5.49

The corresponding bead models are shown in Figs. 4, 5 and 7.
[a] Anhydrous value.
[b] Corrected for hydration (0.4 g water/g protein).
[c] Results obtained with absorbance (Abs) and interference (Int) optics.

more symmetrical and has an $s^{app}_{20,w}$ of just above that for $(p50)_2$; in addition, a minor peak at an $s^{app}_{20,w}$ close to that for IκBγ has appeared. At these ratios it appears that the solution comprises a mixture of uncomplexed $(p50)_2$ and $(p50)_2$–IκBγ complex: the difference in sedimentation coefficients for the two species is small (Table 1) so that analysis with $c(s)$ fails to completely resolve them and results in sedimentation coefficients different from those obtained from a solution monodisperse in one species.

At 1:1 the major peak has narrowed and is centered about a slightly higher $s^{app}_{20,w}$; the minor peak is still apparent. This peak increases in size at 1:2 and further at 1:3, mixing ratios that yield almost identical peaks at the higher $s^{app}_{20,w}$. These overall trends are broadly consistent with the SE data. The true complex is formed when IκBγ is equimolar with p50 or is in excess. Given that the size of the minor peak is so small at the 1:1 ratio, do these data not imply that the ratio of the complex is 2:2? The value for $M_{w,app}$ obtained by SE is too low for such a stoichiometry; given the very small size of the minor peak in the size-distribution analysis, it is not plausible to ascribe a reduction in $M_{w,app}$ to uncomplexed IκBγ. Thus, the SV data also point to a 2:1 stoichiometric complex with $s^0_{20,w} = 5.51 \pm 0.18$ S (absorbance data) or 5.49 ± 0.14 S (interference data).

Sedimentation coefficients were calculated for the 'inhibitor-bound', closed conformation $(p50)_2$–IκBγ complex (Fig. 7) and the 'DNA-bound', open conformation yielding hydrated values of 5.31 and 5.16 S, respectively (Table 1). The closed conformation complex model is more consistent with the experimentally determined sedimentation coefficients. Thus, when the p50 dimer is inhibited by a single IκBγ molecule, it is in the closed conformation.

4. Discussion

Conclusions drawn about the stoichiometry of the complex formed between p50 and IκBγ rely to an extent on certainty of the molar concentrations of the respective proteins. In this sense we were limited by the use of calculated (as opposed to experimentally determined) extinction coefficients. However, we have assessed our findings with this in mind and have critically arrived at the only feasible conclusions, taking into account all of our data. Certainly the 2:1 stoichiometry at which we arrived is consistent with other studies for the interaction of IκBα with NFκB ([14] and references cited therein).

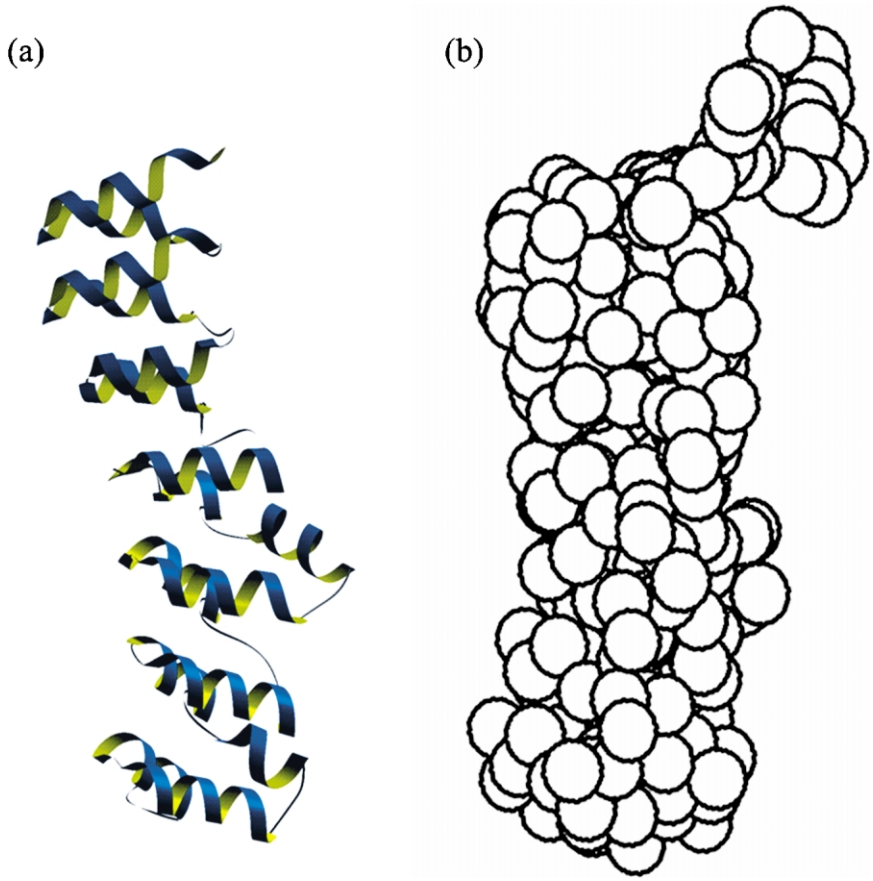

Fig. 5. Models of IκBγ: (a) high-resolution model constructed from the coordinates of IκBα (PDB accession code 1NFI) by attaching a duplicated sixth ankyrin repeat to the molecule's C-terminus; (b) bead model derived from the high-resolution model using the program AtoB [33,34].

In determining the solution conformation of macromolecules, our normal approach is to complement hydrodynamic measurements with small-angle X-ray and/or neutron scattering (SAXS/SANS) data (see e.g. [36–38]). The SAXS data we acquired for IκBγ were dominated at low angles by scattering from aggregates (data not shown here). We observed a steady increase in the scattering at low angles throughout the course of the SAXS data acquisition for IκBγ, indicative of aggregation with time. We do not think that this is necessarily the result of exposure to the X-ray beam because data symptomatic of time-dependent aggregation were also obtained with SE. Although we could have limited our SAXS analysis to early data in which aggregation was not apparent, the statistics of this limited data set were rather poor leading to uncertainties in the subsequent modelling.

Much the same difficulty with SAXS was experienced with p50, although the appearance of aggregate species does appear to be due to radiation damage as it was not observed with AUC. Therefore, we have been unable to determine the solution structures of p50, IκBγ and their complex ab initio.

Comparison of the experimentally determined sedimentation coefficients for p50 (4.19 S (absorbance data) and 4.45 S (interference data)) with those calculated for the two conformations of

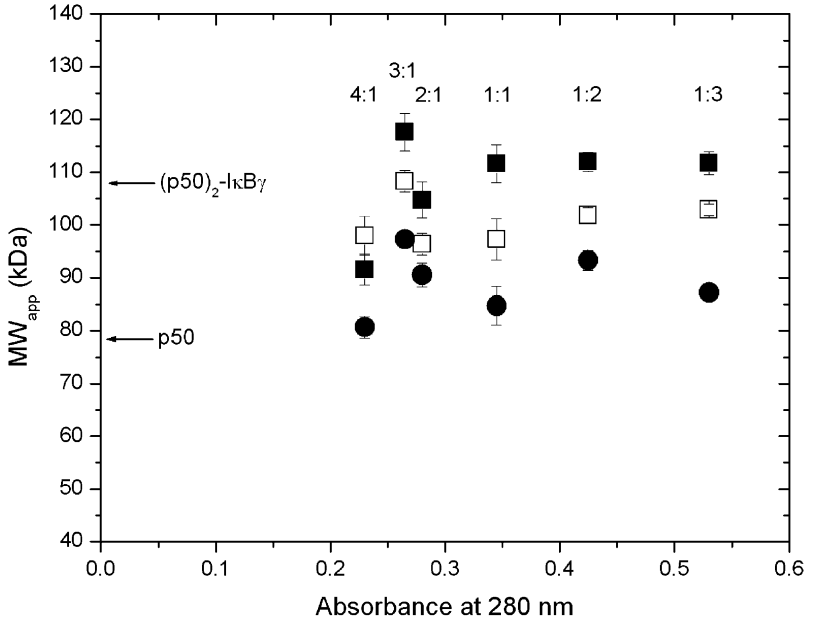

Fig. 6. Apparent whole cell weight average molecular weight ($M_{w,app}$) as a function of loading concentration (in terms of sample absorbance) for mixtures of p50 and IκBγ at molar ratios (p50:IκBγ) of 4:1, 3:1, 2:1, 1:1, 1:2 and 1:3 (data were acquired at rotor speeds of 10 k rpm (filled squares); 13.5 k rpm (open squares); 17 k rpm (filled circles)). For comparison, the molecular weights of p50 dimer and its complex with one molecule of IκBγ are indicated.

dimer (4.03 S in the open and 4.40 S in the closed conformation) suggests that in solution p50 may adopt a conformation intermediate between these two extremes representative of the form taken when inhibitor is bound (closed) and DNA is bound (open); or it may reflect inherent 'floppiness' in the structure: the position of the N-terminal domain of p65 in the crystal structure of the p50–p65 heterodimer complexed with IκBα is partly determined by crystal packing [14]. Nonetheless, it is feasible that by adopting a position intermediate between the two extremes, $(p50)_2$ is poised ready to switch to whichever conformation is appropriate, dependent on the availability of DNA or inhibitor.

The bead model of p50 complexed with IκBγ shows that the modelled-in seventh ankyrin repeat may in fact obstruct the DNA-binding site of p50.

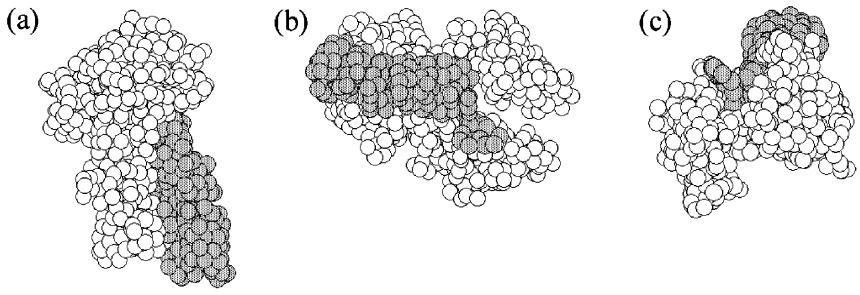

Fig. 7. Orthogonal views of the p50–IκBγ complex bead model in the closed conformation: p50 (white beads); IκBγ (grey beads).

Interestingly, in the complex model the IκBγ C-terminal peptide interacts with the N-terminus of p50. It is tempting to speculate that strong non-covalent interactions between the two make a conformational change in p50 more difficult, possibly explaining why p50 has not been observed to interact with DNA in the presence of IκBγ.

Acknowledgments

The authors are grateful to Ioannis Michalopoulos for his initial work in this area. We also thank Ellis Jaffray for making the p50 and IκBγ used in this study. M.S. is the recipient of a Wellcome Trust Studentship.

References

[1] S. Ghosh, M.J. May, E.B. Kopp, NF-κB and Rel proteins: evolutionarily conserved mediators of immune responses, Annu. Rev. Immunol. 16 (1998) 225.
[2] F. Mercurio, A.M. Manning, Multiple signals converging on NF-κB, Curr. Opin. Cell Biol. 11 (1999) 226.
[3] N.D. Perkins, The Rel/NF-κB family: friend and foe, TIBS 25 (2000) 434.
[4] P. Cramer, C.J. Larson, G.L. Verdine, C.W. Müller, Structure of the human NF-κB p52 homodimer-DNA complex at 2.1 Å resolution, EMBO J. 16 (1997) 7078.
[5] S.Y. Foo, G.P. Nolan, NF-κB to the rescue, TIG 15 (1999) 229.
[6] L. Lin, Cotranslational biogenesis of NF-κB p50 by the 26S proteasome, Cell 92 (1998) 819.
[7] P.A. Baeuerle, IκBα–NFκB structures: at the interface of inflammation control, Cell 95 (1998) 729.
[8] S.G. Sedgwick, S.J. Smerdon, The ankyrin repeat: a diversity of interactions on a common structural framework, TIBS 24 (1999) 311.
[9] H. Ishikawa, D. Carrasco, E. Claudio, R.P. Ryseck, R. Bravo, Gastric hyperplasia and increased proliferative responses of lymphocytes in mice lacking the COOH-terminal ankyrin domain of NF-κB2, J. Exp. Med. 186 (1997) 999.
[10] M. Karin, Y. Ben-Neriah, Phosphorylation meets ubiquitination: the control of NF-κB activity, Annu. Rev. Immunol. 18 (2000) 621.
[11] C.B. Phelps, L.L. Sengchanthalangsy, T. Huxford, G. Ghosh, Mechanism of IκBα binding to NF-κB dimers, J. Biol. Chem. 275 (2000) 29840.
[12] T. Li, L.O. Narhi, J. Wen, et al., Interactions between NFκB and its inhibitor IκB: biophysical characterisation of a NFκB/IκBα complex, J. Prot. Chem. 17 (1998) 757.
[13] S. Malek, T. Huxford, G. Ghosh, IκBα functions through direct contacts with the nuclear localisation signal and the DNA binding sequences of NF-κB, J. Biol. Chem. 273 (1998) 25427.
[14] M.D. Jacobs, S.C. Harrison, Structure of an IκBα/NF-κB complex, Cell 95 (1998) 749.
[15] T. Huxford, D.B. Huang, S. Malek, G. Ghosh, The crystal structure of the IκBα/NF-κB complex reveals mechanisms of NF-κB inactivation, Cell 95 (1998) 759.
[16] F. Arenzana-Seisdedos, J. Thompson, M.S. Rodriguez, F. Bachelerie, D. Thomas, R.T. Hay, Inducible nuclear expression of newly synthesized IκBα negatively regulates DNA-binding and transcriptional activities of NF-κB, Mol. Cell. Biol. 15 (1995) 2689.
[17] M.S. Rodriguez, J. Thompson, R.T. Hay, C. Dargemont, Nuclear retention of IκBα protects it from signal-induced degradation and inhibits nuclear factor κB transcriptional activation, J. Biol. Chem. 274 (1999) 9108.
[18] S. Malek, Y. Chen, T. Huxford, G. Ghosh, IκBβ, but not IκBα, functions as a classical cytoplasmic inhibitor of NF-κB dimers by masking both NF-κB nuclear localisation sequences in resting cells, J. Biol. Chem. 276 (2001) 45225.
[19] S. Bell, J.R. Matthews, E. Jaffray, R.T. Hay, IκBγ inhibits DNA binding of NF-κB p50 homodimers by interacting with residues that contact DNA, Mol. Cell. Biol. 16 (1996) 6477.
[20] Y.Q. Chen, S. Ghosh, G. Ghosh, A novel DNA recognition mode by the NFκB p65 homodimer, Nat. Struct. Biol. 5 (1998) 67.
[21] F.E. Chen, D.B. Huang, Y.W. Chen, G. Ghosh, Crystal structure of the p50/p65 heterodimer of transcription factor NF-κB bound to DNA, Nature 373 (1998) 410.
[22] G. Ghosh, G.V. Duyne, S. Ghosh, P.B. Sigler, Structure of NF-κB p50 homodimer bound to a κB site, Nature 373 (1995) 303.
[23] C.W. Müller, F.A. Rey, M. Sodeoka, G.L. Verdine, S.C. Harrison, Structure of the NF-κB p50 homodimer bound to DNA, Nature 373 (1995) 311.
[24] F. Michel, M. Soler-Lopez, C. Petosa, P. Cramer, U. Siebenlist, C.W. Müller, Crystal structure of the ankyrin repeat domain of Bcl-3: a unique member of the IκB protein family, EMBO J. 20 (2001) 6180.
[25] J.R. Matthews, N. Wakasugi, J.-L. Virelizier, J. Yodoi, R.T. Hay, Thioredoxin regulates the DNA binding activity of NF-κB by reduction of a disulphide bond involving cysteine 62, Nucleic Acids Res. 20 (1992) 3821.
[26] J.R. Matthews, E.A. Watson, S.L. Buckley, R.T. Hay, Interaction of the C-terminal region of p50 with the nuclear localisation signal of p50 is required for inhibition of NF-κB DNA binding activity, Nucleic Acids Res. 21 (1993) 4516.
[27] U.K. Laemmli, Cleavage of structural proteins during the assembly of the head of bacteriophage T4, Nature 227 (1970) 680.
[28] P. Schuck, Size-distribution analysis of macromolecules by sedimentation velocity ultracentrifugation and Lamm equation modeling, Biophys. J. 78 (2000) 1606.

[29] H.M. Berman, J. Westbrook, Z. Feng, et al., The protein data bank, Nucleic Acids Res. 28 (2000) 235.
[30] N. Guex, M.C. Peitsch, SWISS-MODEL and the Swiss-Pdb Viewer: an environment for comparative protein modelling, Electrophoresis 18 (1997) 2714.
[31] J.A. Cuff, M.E. Clamp, A.S. Siddiqui, M. Finlay, G.J. Barton, JPRED: a consensus secondary structure prediction server, Bioinformatics 14 (1998) 892.
[32] A. Aszódi, W.R. Taylor, Folding polypeptide alpha-carbon backbones by distance geometry methods, Biopolymers 34 (1994) 498.
[33] O. Byron, Construction of hydrodynamic bead models from high-resolution X-ray crystallographic or nuclear magnetic resonance data, Biophys. J. 72 (1997) 408.
[34] O. Byron, Hydrodynamic bead modelling, Methods Enzymol. 321 (2000) 278.
[35] J. García de la Torre, S. Navarro, M.C. Lopez Martinez, F.G. Díaz, J.J. Lopez Cascales, HYDRO: a computer program for the prediction of hydrodynamic properties of macromolecules, Biophys. J. 67 (1994) 530.
[36] A.S. Solovyova, N. Meenan, L. McDermott, et al., The polyprotein and FAR lipid binding proteins of nematodes: shape and monomer/dimer states in ligand-free and bound forms, Eur. Biophys. J. 32 (2003) 465.
[37] C.J. Ackerman, M.M. Harnett, W. Harnett, D.I. Svergun, O. Byron, 19 Å solution structure of the filarial nematode immunomodulatory protein, ES-62, Biophys. J. 84 (2003) 489.
[38] D.J. Scott, J.G. Grossmann, J.R.H. Tame, O. Byron, K.S. Wilson, B.R. Otto, Low resolution structure of the apo form of *Escherichia coli* haemoglobin protease Hbp, J. Mol. Biol. 315 (2002) 1179.